Kinetic Mechanism of L-α-Glycerophosphate Oxidase from *Mycoplasma pneumoniae*

Somchart Maenpuen[1], Pratchaya Watthaisong[1], Pacharee Supon[1], Jeerus Sucharitakul[2], Derek Parsonage[3], P. Andrew Karplus[4], Al Claiborne[3]and Pimchai Chaiyen[5]*

[1]Department of Biochemistry, Faculty of Science, Burapha University, 169 Long-Haad Bangsaen Road, Chonburi, 20131, Thailand

[2]Department of Biochemistry, Faculty of Dentistry, Chulalongkorn University, Henri-Dunant Road, Patumwan, Bangkok 10330, Thailand

[3]Department of Biochemistry and Center for Structural Biology, Wake Forest School of Medicine, Winston-Salem, North Carolina 27157, United States

[4]Department of Biochemistry and Physics, Oregon State University, Corvallis, Oregon 97331, United States

[5]Department of Biochemistry and Center of Excellence in Protein Structure & Function, Faculty of Science, Mahidol University, Rama 6 Road, Bangkok, 10400, Thailand

*Correspondence to: P. Chaiyen, Department of Biochemistry and Center of Excellence in Protein Structure & Function, Faculty of Science, Mahidol University, Rama 6 Road, Bangkok, 10400, Thailand. Fax: +6623547174, Tel: +6622015596,

Email: pimchai.cha@mahidol.ac.th

Running Title

Catalytic properties of L-α-glycerophosphate oxidase from *Mycoplasma pneumoniae*

Abbreviations

His_6-*Mp*GlpO, six-histidine-tagged *Mycoplasma pneumonia* L-α-glycerophosphate oxidase; FAD, flavin adenine dinucleotide; Glp, L-α-glycerophosphate; DHAP, dihydroxyacetone phosphate; GAP, DL-glyceraldehyde 3-phosphate; H_2O_2, hydrogen peroxide; ABTS, 2,2'-azino-bis(3-ethylbenzothiazoline-6-sulfonic acid) diammonium salt; HRP, horseradish peroxidase.

Enzyme Commission number

L-α-glycerophosphate oxidase, EC 1.1.3.21

Keywords

L-α-glycerophosphate oxidase;flavoprotein oxidase;flavin adenine dinucleotide (FAD);transient kinetics; *Mycoplasma pneumoniae*

Subdivision

Enzymology

Abstract

L-α-glycerophosphate oxidase is an FAD-dependent enzyme that catalyzes the oxidation of L-α-glycerophosphate (Glp) by molecular oxygen to generate dihydroxyacetone phosphate (DHAP) and hydrogen peroxide (H_2O_2). The catalytic properties of the recombinant His_6-GlpO from *Mycoplasma pneumoniae*(His_6-*Mp*GlpO) were investigated with transient and steady-state kinetics and ligand binding. The results indicate that the reaction mechanism of His_6-*Mp*GlpO follows a ping-pong model. Double-mixing stopped-flow experiments show that after flavin-mediate substrate oxidation, DHAP leaves rapidly prior to the oxygen reaction. The values of the individual rate constants and k_{cat} (4.2 s^{-1}at 4 ^oC) determined, in addition to the finding that H_2O_2 can bind to the oxidized enzyme suggest that H_2O_2 release is the rate-limiting step for the overall reaction. Results indicate that His_6-*Mp*GlpO contains mixed populations of fast and slow reacting species. Only the fast reacting species predominantly participates in turnovers. Different from other GlpO enzymes previously reported, His_6-*Mp*GlpO can catalyze the reverse reaction of reduced enzyme and DHAP. This result can be explained by the standard reduction potential value of His_6-*Mp*GlpO(-167 ± 1 mV), which is lower than those of GlpO from other species. We found that DL-glyceraldehyde 3-phosphate(GAP)can be used as a substrate in the His_6-*Mp*GlpO reaction, although it exhibited a ~100-fold lower k_{cat} value in comparison to the reaction of Glp. These results also imply the involvement of GlpO in glycolysis, as well as in lipid and glycerol metabolism. The kinetic models and distinctive properties of His_6-*Mp*GlpO reported here should be useful for future studies of drug development against *Mycoplasma pneumonia* infection.

Introduction

L-α-glycerophosphate oxidase (GlpO) is a flavoprotein oxidase containing FAD as a cofactor. The enzyme catalyzes the oxidation of L-α-glycerophosphate (Glp)– a metabolic intermediate in lipid biosynthesis, glycolysis, and glycerol metabolism–at the C2 position to yield dihydroxyacetone phosphate (DHAP) as a product. Molecular oxygen (O_2) acts as an electron acceptor in this reaction by receiving two electrons from the substrate to generate hydrogen peroxide (H_2O_2) [1-5]. H_2O_2 is a reactive oxygen species (ROS) that can be converted to more potent reactive oxygen species such as peroxide or hydroxyl radicals and H_2O_2 itself can also serve as a cellular signaling molecule [6]. ROS can affect cell viability by causing lysis of red blood cells, lipid peroxidation, and other oxidative damage [7,8]. The GlpO reaction in *Mycoplasma pneumonia* has been shown to play a role in the virulence of the bacteria, which presents itself as infection of the human respiratory tract[4, 5, 8, 9]. It is thought that H_2O_2 produced from this reaction is involved in the pathogenicity of pneumonia.

GlpO from several bacteria have been studied. Due to its absence in mammalian cells, this enzyme has been proposed as a target for new antibiotic development [10]. Native GlpO from *Trypanosoma brucei*, a human parasite that causes an African sleeping sickness, was isolated, purified and studied with regards to its inhibition. Results indicate that suramin, melarsen oxide, salicylhydroxamic acid, 3-chlorobenzylhydroxamate, 8-hydroxyquinoline, and alkyl esters of 3,4-dihydroxybenzoate are potent inhibitors for GlpO from *T. brucei*[10-14]. GlpO from lactic acid bacteria such as *Streptococcus* sp. and *Streptococcus faecium* ATCC 12755 were also studied [2, 3]. Investigations on the inhibition of the enzyme showed that *S. faecium* GlpO could be inhibited by fructose 6-

phosphate [2]. Besides oxygen, the *S. faecium* enzyme can also use other compounds such as ferricyanide and dichlorophenol indolephenol (DCPIP) as electron acceptors[3]. Studies of the recombinant GlpO from *Enterococcus casseliflavus* indicate that the reaction obeys a ping-pong kinetics model and that the flavin reduction step is the rate-limiting step for the overall turnover [15]. In contrast, kinetic studies of the wild-type GlpO from *Streptococcus* sp. and the mutant enzyme in which a flexible surface region was truncated indicate that DHAP release is the rate-limiting step of the reaction [16]. Crystal structures of both wild-type and truncated mutant of *Streptococcus* sp. GlpO at 2.4 and 2.3 Å resolution, respectively were solved. The data indicate that the active site residues in *Streptococcus* sp. GlpO that may be involved in Glp substrate binding are mostly positively charged residues such as Arg346, Lys429, His65, and Arg69 [17, 18].

In this work, the biochemical and catalytic properties of a new GlpO from *Mycoplasma pneumonia* was investigated using steady-state and transient kinetics, and ligand binding studies. The enzyme shows several unique catalytic properties that have never been reported for other enzymes. It can catalyze a reverse flavin oxidation using the reaction product, DHAP as an electron acceptor. In contrast to previously investigated systems, the rate-limiting step of *Mycoplasma* GlpO is likely the release of H_2O_2 because other reaction steps are faster than the catalytic turnover number. Besides Glp, the enzyme can also use glyceraldehyde 3-phosphate (GAP), an intermediate in the glycolysis pathway, as a substrate, implying that the H_2O_2 generated by the GlpO reaction in *Mycoplasma pneumoniae* can be derived from lipid, glycerol and sugar metabolism.

Results

Preparation and spectroscopic properties of His_6-MpGlpO

Recombinant His_6-*Mp*GlpO was successfully expressed as a soluble enzyme in *E. coli* BL21(DE3) cells cultured in Terrific Broth and induced by IPTG at 25 ^{o}C. The yield of cell paste was about 17 g per 1 liter of cell culture. His_6-*Mp*GlpO was purified to homogeneity using Ni-Sepharose affinity and SP-Sepharose cation-exchange chromatography as described in Experimental Procedures. This protocol resulted in ~19 mg of purified enzyme with a specific activity of ~10 U/mg per 1 liter of cell culture (Table 1). A low yield of the enzyme preparation was due to the protein loss during the last step (SP-sepharose chromatography). This step was used because it could remove impurities that were retained after Ni-Sepharose chromatography. SDS-PAGE (12%) analysis indicated that the enzyme is >95% pure and that the subunit molecular mass was about 43 kDa (data not shown). The purified enzyme exhibited spectral characteristics typical of FAD-bound enzyme with a maximum absorbance at 448 nm (solid line of Fig. 1). The molar absorption coefficient was determined according to the protocol described in Experimental Procedures as 12.40 ± 0.03 $mM^{-1}cm^{-1}$, which is slightly different from a molar absorption coefficient of free-released FAD (11.3 $mM^{-1}cm^{-1}$) (dashed line of Fig. 1).

Steady-state kinetics of His_6-MpGlpO

The two-substrate steady state kinetics of His_6-*Mp*GlpO using Glp and O_2 as substrates was investigated at 4 ^{o}C, pH 7.0 using the 2,2'-azino-bis(3-ethylbenzothiazoline-6-sulphonic acid)-horse radish peroxidase (ABTS-HRP) coupled

assay system as described in Experimental Procedures. Initial rates of reactions at various concentrations of Glp and O_2 were measured. A double-reciprocal plot of initial rates and concentrations, e/v_o *versus* 1/[Glp] (Fig. 2A) or 1/[O_2] (Fig. 2B), showed parallel lines, indicating that the His_6-*Mp*GlpO reaction uses a ping-pong mechanism. Steady-state kinetic parameters of the enzyme reaction that were obtained from reciprocal (Eqn 2) or direct plots (Eqn 3) were similar: K_m^{Glp}, 5.5 ± 0.4 mM; $K_m^{O_2}$, 55±8μM; and k_{cat}, 4.2 ± 0.1 s^{-1} at 4 °C. The results indicated that the steady-state turnover number of GlpO from *M. pneumoniae* is about 4- and 9-fold lower than that of GlpO from *Streptococcus* sp. (18 s^{-1}) and *Enterococcus casseliflavus* (37 s^{-1}), respectively [15, 16].

Standard reduction potential value of His_6-MpGlpO

The standard reduction potential value of His_6-*Mp*GlpO was measured by Massey's method using cresyl violet as a reference dye. Spectra obtained during the reduction (Fig. 1B) indicated that the enzyme was completely reduced via a two-electron reduction process using the benzyl viologen-mediated xanthine/xanthine oxidase system. Concentrations of the oxidized enzyme and the reduced dye were calculated based on their absorbance at 407 and 540 nm, respectively. The standard reduction potential value (E_e^0) of the enzyme was calculated from the y-intercept of the plot of $\log(E_{red}/E_{ox})$ *versus* $\log(D_{red}/D_{ox})$ as -167 ± 1 mV (Inset of Fig. 1B).

Kinetics of the reduction of His_6-MpGlpO by Glp

A solution of the oxidized enzyme (~28 μM after mixing) in 50 mM sodium phosphate buffer, pH 7.0 containing 0.5 mM EDTA, and 1 mM DTT was mixed with

various concentrations of Glp under anaerobic conditions, and the kinetics of enzyme reduction was monitored by the change in absorbance at 448 nm using a stopped-flow spectrophotometer at 4 ^{o}C. Kinetic traces shown inFig. 3A indicate that flavin reduction shows biphasic kinetics in which the amplitude change of the first (fast) phase varied from 10-70% (relative to total flavin reduction) while the second (slow) phase was from 90-30% upon increasing the concentration of Glp. This indicates that there are two distinct populations of the oxidized enzyme that are slowly interconverted. The k_{obs} values obtained from both phases are hyperbolically dependent on Glp concentration (Figs. 3B and 3C). According to the plots, the reduction rate constants (k_{red}) were determined as 199 ± 34 and 2.08 ± 0.01 s^{-1}, respectively. Because k_{obs} of both phases were hyperbolically dependent on substrate concentration (Figs. 3B and 3C), the data suggest that each of the oxidized enzyme forms reacts with Glp via a two-step reduction process in which a binary complex of the oxidized enzyme and its substrate is initially formed in the first step, followed by flavin reduction in the second step (Fig. 3E). These data indicate that the substrate binding affinity of the fast reacting species (K_d = 72 ±18mM) is 52-fold lower than that of the slow reacting enzyme (K_d = 1.38 ± 0.02mM). As at the highest concentration of Glp where both populations of enzyme can react with Glp rapidly, the amplitude ratio of fast:slow species is 70:30, the data indicate that a ratio of fast to slow species under equilibrium is 70:30. This conclusion is also supported by the results of the oxidative half-reaction (see the following section). We also noted that a clear amplitude change ratio of 70:30 could only be observed when the k_{obs} value of the fast reacting species is ≥16 s^{-1}. These results also imply that k_f+ k_r of the interconversion process between the fast and slow reacting species is <16 s^{-1}(Fig. 3E).

Kinetics of the reaction of reduced His_6-MpGlpO with O_2

An anaerobic solution of the reduced enzyme (~28 μM after mixing) in 50 mM sodium phosphate buffer, pH 7.0 containing 0.5 mM EDTA, and 1 mM DTT was mixed with buffer containing various concentrations of oxygen. The kinetics of enzyme oxidation was monitored by measuring the absorbance at 448 nm using a stopped-flow spectrophotometer at 4 ^{o}C. Kinetic traces for enzyme oxidation are biphasic (Fig. 4A) in which the amplitude change for the first (fast) phase reflects 70% of the total amount of flavin oxidation while the second (slow) phase is about 30%. Some fraction of the fast reacting enzyme was oxidized during the dead-time period. Kinetic analyses indicate that the k_{obs} values of the first phase and second phase *versus* the oxygen concentration are hyperbolic, with rate constant values for the fast and slow reacting species of 627 ± 81 and 85 ± 11 s^{-1}, respectively (Figs. 4B and 4C). The hyperbolic plots obtained for the k_{obs} values *versus* oxygen concentration suggest that the re-oxidation occurs via a two-step process. The reduced enzyme may form a binary complex with O_2 prior to flavin re-oxidation in the second step. According to the plots shown in Figs. 4B and 4C, the K_d values for binary complex formation were 1.3 ± 0.2 and 0.5 ± 0.1 mM for the fast and slow reacting enzyme species, respectively. Similar to the reductive half-reaction, the ratio of amplitude of fast to slow reacting species is 70:30. The amplitude changes observed due to the fast and slow reacting species was clearly separated at all oxygen concentrations employed because all k_{obs} values were greater than 16 s^{-1} (the lowest k_{obs} value in Fig. 4C is 17.6 s^{-1}). The kinetic mechanism of the oxidative half-reaction is summarized in Fig. 4D.

Effects of DHAP on the oxidative half-reaction of His_6-MpGlpO

Previous studies of the reductive half-reaction (Fig. 3A) indicated that the reduction of enzyme by Glp is a fast process in which DHAP release cannot be detected in the stopped-flow experiments. In this experiment, we used double-mixing stopped-flow experiments (see Experimental Procedures) to investigate if DHAP can bind to the reduced enzyme by monitoring the influence of DHAP on the oxidative half-reaction. The reduced enzyme was mixed with an equal concentration of Glp and aged for 100 s (to ensure complete reduction) in the first mixing step. The DHAP-bound reduced enzyme was then mixed with various concentrations of O_2 in the second mixing step and the enzyme re-oxidation was followed by monitoring the absorbance at 448 nm, similar to the experiments in Fig. 4A. The kinetic traces obtained from the change in absorbance at 448 nm shown in Fig. 5A display biphasic kinetic and amplitude changes for the first (70%) and second (30%) phases similar to those observed for the oxidative half-reaction carried out using the single-mixing mode in Fig. 4A(Fig. 5A). Kinetic analyses also indicate that the k_{obs} values for both phases and the rate constants for enzyme oxidation (k_{ox} = 524 ± 34 s^{-1}(Fig. 5B) and 107 ± 5 s^{-1}(Fig. 5C)), are similar to those obtained from Fig. 4 (627 ± 81 s^{-1}(Fig. 4B) and 85 ± 11 s^{-1}(Fig. 4C)). The similarities in the kinetic results obtained by the two different mixing modes suggest that after the enzyme was reduced by Glp, the DHAP formed was quickly released prior to the reaction of the reduced enzyme with oxygen.

To verify our hypothesis, the reduced enzyme (91 μM before mixing) plus DHAP (136.5 μM before mixing) was incubated for various aging times in the first mixing step. The solution was then mixed with buffer containing oxygen at 0.26 mM (before mixing)

in the second mixing step to allow the re-oxidation of enzyme to occur while the progression of the reaction was monitored by measuring the absorbance change at 448 nm. Analyses of the kinetic traces (Fig. 5D) indicated that the k_{obs} values and the amplitude changes obtained from various age times were similar and also similar to those obtained from the previous results (Fig. 5A). These data again suggest that DHAP does not tightly bind to the enzyme but rather, was quickly released after its formation. All results indicate that the reaction of His_6-*Mp*GlpO occurs via a true ping-pong mechanism.

Product binding and the reverse oxidation of reduced His_6-MpGlpO by DHAP

Both the oxidized and reduced forms of the enzyme were tested for their ability to bind various ligands by detecting their absorbance signal changes (Experimental Procedures). For the binding of the oxidized enzyme and H_2O_2, a solution of oxidized enzyme (24 μM) was titrated in various concentrations of H_2O_2. The difference spectra (data not shown) indicated a maximum absorbance change at 385 nm. The equilibrium dissociation constant (K_d) determined from measurements at 385 nm for the binding of H_2O_2 to the oxidized enzyme was determined as 0.4 ± 0.2 mM. The same experiment was also performed using DHAP at various concentrations. The difference spectra obtained did not show any clear signal due to the binding of oxidized enzyme and DHAP. The large absorption increase at shorter wavelengths was likely due to DHAP absorption (data not shown). As H_2O_2 can bind to the oxidized enzyme, H_2O_2 release from the enzyme may be a rate-limiting step for the overall catalytic turnover of the enzyme reaction.

Results from the addition of DHAP at various concentrations to the reduced His_6-*Mp*GlpO (24 μM) indicate that the reduced enzyme can be re-oxidized by DHAP (Fig. 6A), suggesting that the reduction of His_6-*Mp*GlpO by Glp is reversible. Therefore, the kinetics of re-oxidation of the reduced enzyme with DHAP was investigated by monitoring the absorbance change at 448 nm using single-mixing mode stopped-flow spectrophotometry (Experimental Procedures). The kinetic traces at 448 nm (Fig. 6B) showed biphasic kinetics with majority of absorbance increase in the second phase. Kinetic analyses showed that the k_{obs} values obtained from the first phase were independent of DHAP concentration with values ~6 s^{-1} (Fig. 6C), while those obtained from the second phase are linearly dependent on DHAP concentration with a bimolecular rate constant of 56.5 $M^{-1}s^{-1}$(Fig. 6D). As the first reaction of reduced GlpO and DHAP is a bimolecular reaction in which the rate constants should be linearly dependent on DHAP, these results suggest that the rate constant (6 s^{-1}) observed in the first phase likely belongs to the step following the bimolecular reaction. Due to its greater value than the k_{obs} values of the bimolecular reaction of reduced enzyme and DHAP, this step appeared at the first phase even though it in fact occurs after the initial bi-molecular reaction (rate-switching phenomenon, [19]). The kinetic model of the reaction of reduced enzyme with DHAP to form the oxidized enzyme and Glp is shown in Fig. 6E.

Overall catalytic reaction of His_6-MpGlpO

Based on the results of transient and steady-state kinetic studies shown in Figs. 2-4, the overall reductive and oxidative half-reactions of His_6-*Mp*GlpO can be summarized as shown in Fig 7. Both half-reactions showed evidence supporting the presence of a

mixture of fast and slow reacting enzymes, present at a molar ratio of 70:30. As the overall k_{cat} derived from the steady-state kinetic measurements was 4.2 s^{-1} and the k_{red} value of the slow reacting species (upper path, Fig. 7) was 2.08 ± 0.01 s^{-1}(Fig. 3C), the results indicated that primarily, only the fast reacting species is involved in the reductive half-reaction during the catalytic turnover. Because all of the rate constants measured had greater values than the k_{cat}, we propose that the rate-limiting step is associated with product release. As the results from the double-mixing experiments in Fig. 5 indicated that DHAP release is rapid, we thus propose that the release of H_2O_2 is the rate-limiting step of the overall reaction.

Data obtained from the reverse reaction of His_6-*Mp*GlpO are useful for assigning the rate constants in the reductive half-reaction. The results in Figs. 6C and 6D were used to assign rate constants for the bimolecular reaction between reduced enzyme and DHAP as 56.5 $M^{-1}s^{-1}$ and for the dissociation of Glp from the E_{ox}:Glp binary complex as 6 s^{-1}(red arrows in Fig. 7). As the reverse reaction (Figs. 6) only showed ~80% of the reduced enzyme oxidation at the end, the data imply that only the reaction of fast reacting species was observed (rate 56.5 $M^{-1}s^{-1}$, red arrow of Fig. 7). This suggests that the rate constant of 6 s^{-1} is likely k_2 of the first step in Fig. 7. Therefore, based on a K_d value of 72 mM (the first step), k_1 can be calculated as 83.3 $M^{-1}s^{-1}$.

Glyceraldehyde 3-phosphate can be used as a substrate for the His_6-MpGlpO reaction

As the previous report showed that a significant amount of H_2O_2 could be generated in *M. pneumoniae* when glucose (0.1 mM) was used as a sole carbon source [5] and the structure of GAP (an intermediate in the glycolytic pathway) is similar to Glp, we

investigated whether GlpO can use GAP as a substrate. Apparent steady state kinetics of the His_6-*Mp*GlpO reaction using GAP as a substrate under air-saturation (0.26 mM) was measured. The reactions were carried out at 25 ^{o}C, pH 7.0 using the same ABTS-HRP assay at various concentrations of GAP (0.025-6.4 mM) (Experimental Procedures). The results show that GAP can be used as a substrate for His_6-*Mp*GlpO. Initial rates were directly plotted as a function of GAP concentration (Fig. 3D). For comparison, similar reactions with Glp as a substrate were carried out under the same conditions. The results clearly indicate that His_6-*Mp*GlpO can use GAP as a substrate. The apparent steady-state kinetic parameters were as follows: K_m^{GAP}, 1.8 ± 0.2 mM; k_{cat},0.6 s^{-1}, and k_{cat}/K_m, 0.33 $mM^{-1}s^{-1}$. When compared to the kinetic parameters of Glp, it is quite clear that the enzyme prefers to use Glp as a substrate because the k_{cat} and k_{cat}/K_m of the Glp reactions are 100- and 15-fold larger than those of the GAP reactions, respectively (Inset of Fig. 13) (K_m^{Glp}, 12 ± 1 mM; k_{cat},60.1 s^{-1}, and k_{cat}/K_m,5 $mM^{-1}s^{-1}$). Nevertheless, our data imply that in the absence of glycerol, GAP may serve as a substrate in the GlpO reaction to supply H_2O_2 during mycoplasma infection.

Ligand Binding

The bindings of the oxidized enzyme with other ligands (glycerol, L-lactate, and DL-malate) were investigated to gain the understanding on the active site specificity. Results indicate that only the binding of the oxidized enzyme with L-lactate and DL-malate, not glycerol, can give clear spectroscopic changes (data not shown). The K_d values of the binding of the oxidized enzyme and L-lactate calculated from absorbance changes at 401 and 489 nm are 23 ± 4 and 26 ± 4 mM, respectively. For the binding of

enzyme and DL-malate, the K_d value determined based on absorbance changes at 440 nm is 10 ± 5 mM. These data suggest that enzyme can bind to these substrate analogues but with low affinity.

Discussion

Our work herein reports on the biochemical and catalytic properties of the recombinant GlpO from *Mycoplasma pneumoniae*. The enzyme is unique among all GlpO enzymes for its ability to catalyze the reverse reaction of reduced enzyme and DHAP. The results also showed that besides Glp, GlpO can also use GAP as a substrate. His_6-*Mp*GlpO was successfully expressed in a soluble form in *E. coli*, giving a protein yield of around 19 mg/L cell culture. The purified enzyme has a specific activity of about 10 U/mg, and exhibits biochemical properties similar to other flavoprotein oxidases. The His_6-*Mp*GlpO-bound FAD has a maximum absorption at 448 nm with a molar extinction coefficient of 12.40 $mM^{-1}cm^{-1}$(Fig. 1A). These values are slightly different from those of free FAD (11.3$mM^{-1}cm^{-1}$ at 450 nm) [20], and GlpO from *Streptococcus faecium* (11.3 $mM^{-1}cm^{-1}$ at 446nm) [3] and *Streptococcus* sp. (11.2 $mM^{-1}cm^{-1}$ at 449 nm) [16].

Unlike other GlpO enzymes previously investigated such as the enzyme from *S. faecium* [3], His_6-*Mp*GlpO can catalyze the reverse reaction of reduced enzyme and DHAP. This catalytic property of His_6-*Mp*GlpO may represent a control mechanism to prevent excessive generation of H_2O_2, which may be harmful to bacterial cells. Based on the rate constants determined in Fig. 7 and Table 2, the data indicate that the rate constants of the forward reaction (black arrows) are much greater than the reverse reaction (red arrows). Therefore, the reverse reaction can only occur at very high DHAP

concentrations. Similar to GlpO, another flavoenzyme mandelate dehydrogenase (MDH) was also reported to catalyze the reverse flavin oxidation by the product [21].

The ability of His_6-*Mp*GlpO to accept electrons from DHAP can also be explained by the reduction potential (E_m^0) of enzyme-bound FAD (FAD/$FADH_2$). The E_m^0 value of His_6-*Mp*GlpO (Fig. 1B) was calculated as -167 ± 1 mV which is lower than the value of GlpO from *Enterococcus casseliflavus* (-118 mV) [15]. With the reduction potential of DHAP/Glp of -190 mV, the change of the standard reduction potential ($\Delta E^{o\prime}$) for the forward reaction of His_6-*Mp*GlpO (FAD + Glp→ $FADH_2$ + DHAP) is +23 mV, which corresponds to a standard free-energy change ($\Delta G^{o\prime}$) of -4.44 kJ/mol. Based on these parameters, Glp can favorably reduce the His_6-*Mp*GlpO-bound FAD and the reverse reaction can occur at high concentrations of DHAP (such as those used in Fig. 6A). For GlpO from *E. casseliflavus* that has an E_m^0 value of -118 mV, the thermodynamics of the forward reduction reaction of this enzyme is more heavily favored than the reverse reaction. The reverse reaction of FAD oxidation by DHAP would require much higher concentrations of DHAP than those employed in the previous investigation [3].

Steady-state kinetic analysis of the His_6-*Mp*GlpO reaction using Glp and O_2 as substrates indicates that the reaction obeys ping-pong kinetics with a turnover number (k_{cat}) of 4.2 s^{-1}(Fig. 2). This k_{cat} value is 4- and 9-fold lower than those of GlpO from *Streptococcus* sp. (18 s^{-1}) [16] and *E.casseliflavus* (37 s^{-1}) [15] under the same pH (7.0) and temperature (4-5 ^{o}C), respectively. These enzymes also use a ping-pong mechanism for their reactions. The K_m value for Glp in the His_6-*Mp*GlpO reaction is 5.5 mM, which is about 4-fold lower and 3-fold higher those of GlpO from *E.casseliflavus* (24 mM) [15] and *Streptococcus* sp. (2 mM) [16], respectively. However, these enzymes have K_m

values of O_2 in the same range. The K_m of oxygen for His$_6$-*Mp*GlpO is 55 µM while those for the enzymes from *E.casseliflavus* and *Streptococcus* sp. are 35 µM and 52 µM, respectively [15, 16].

As for the relevance of these kinetic parameters under physiological conditions, the K_m value for Glp in the *M. pneumoniae* GlpO reaction (5.5 mM) is much higher than the physiological concentration of Glp in *M. pneumoniae* (~0.1 mM). The Kd value of the fast reacting (72 mM) that was obtained from half-saturation of kobs is also much higher than the range of Glp physiological concentration. We estimated the physiological concentration of Glp based on the concentration of glycerol present in the host blood serum [5, 8] because a previous investigation on glycerol and Glp uptake in *M.mycoides* SC showed that only glycerol, not Glp, could be taken up into the cells. Glycerol can be converted to Glp by intracellular glycerol kinase [22]. Altogether, these data imply that under physiological conditions, GlpO only functions at a slow rate (turnover≈0.72 s^{-1}).

Our investigation also suggests that besides its physiological substrates, His$_6$-*Mp*GlpO can use GAP as an electron donor (Fig. 3D), although with the k_{cat} value ~100-fold lower than Glp. These results suggest that GAP, a metabolic intermediate in the glycolysis pathway, may also be involved in H_2O_2 production during mycoplasma infection. Therefore, GlpO can be viewed as an enzyme that can employ substrates from three metabolic pathways (the glycerol and lipid metabolic pathways, and glycolysis) for the generation of the reactive oxygen species necessary for the virulence of *M. pneumoniae*. His$_6$-*Mp*GlpO can use a variety of compounds such as 2,6-dichlorophenol indole phenol (DCPIP), phenazinemethosulfate (PMS) and menadione as electron acceptors (data not shown). This is similar to GlpO from *S.faecium* that can use

ferricyanide and DCPIP as electron acceptors [3]. These data imply that if oxygen is not readily available in the cells, the GlpO reactions may mediate the transfer of electrons from Glp or GAP to other mediators such as quinones for cell energy production.

Investigation of binding of His_6-*Mp*GlpO with ligands gives insight into specificity of the active site. Our data indicate that His_6-*Mp*GlpO can bind L-lactate and DL-malate, but not glycerol. Previous study of GlpO from *S. faecium* ATCC12755 also showed that the enzyme could be inhibited by fructose 6-phosphate [2]. These results suggest that the interaction between the anionic moiety of ligand with the enzyme active site is important for the ligand anchorage. Previous structural analysis of a truncated form of GlpO from *Streptococcus* sp. (*Ssp*GlpOΔ) [18] indicates that the Glp-binding pocket of *Ssp*GlpOΔ is formed by various positively charged residues such as Lys429, His65, Arg69, and Arg346. The Arg346 in *Ssp*GlpOΔ is equivalent to Arg302 in glycine oxidase (ThiO) and Arg285 in yeast D-amino acid oxidase (DAAO) [18]. The guanidinium side chain of Arg in these enzymes interacts with a carboxylate group of amino acid substrates. Concurrent with the work in this report, the X-ray structures of His_6-*Mp*GlpO in both oxidized and reduced forms were solved at 2.4 and 2.5 Å resolutions, respectively. More details about His_6-*Mp*GlpO structure and interactions with ligands can be found in [23]. The currently available structures suggest that Arg320 of *Mp*GlpO is important for substrate recognition because its guanidinium side chain shows electrostatic interaction with the phosphate moiety of Glp. The data also show that the α-carboxyl moiety of Gly259 and β-hydroxyl moiety of Ser348 can make a hydrogen bond interaction with the C1-OH and C2-OH of Glp, respectively. His51 is located at the position in which it can act as a base to deprotonate the C2-OH of Glp to initiate the hydride transfer for the

flavin reduction [23]. These residues are also likely to be important for providing the protein-ligand interaction with GAP.

A mixture of fast and slow reacting species observed in the reaction of His_6-*Mp*GlpO was also observed in GlpO from *E. casseliflavus* (*Ec*GlpO) [15] and *Streptococcus* sp. (*Ssp*GlpO) [16]. For *Ec*GlpO reduction, the first (fast) phase was hyperbolically dependent on Glp concentration with a limiting k_{red} value of 48 s^{-1}, while the second (slow) phase was independent of Glp concentration with invariable rate constant values of 3.6-5.4 s^{-1}[15]. In contrast to His_6-*Mp*GlpO and *Ec*GlpO, the first (fast) phase of the *Ssp*GlpO reduction reaction is linearly dependent on the Glp concentration, with a bimolecular rate constant for enzyme reduction of 4900 M^{-1} s^{-1}. On the other hand, the second (slow) phase was independent of Glp concentration with an invariable rate constant value of 11.7 s^{-1} [16]. Similar to His_6-*Mp*GlpO, the reduction rate constant of the slow reacting species of both enzymes is significantly lower than that of their overall turnovers, suggesting that the fast reacting enzymes is primarily responsible for the catalytic reactions.

In contrast to many flavin-dependent enzymes that use oxygen as a substrate, a plot of k_{obs} for the enzyme oxidation *versus* oxygen was hyperbolic. This reaction does not form C4a-hydroperoxyflavin as in the reaction of pyranose 2-oxidase [24, 25] or *p*-hydroxyphenylacetate hydroxylase [26, 27]. The origin of the His_6-*Mp*GlpO hyperbolic dependency on oxygen concentration is not certain. Although a simple kinetic interpretation would allude to the formation of a binary complex of reduced enzyme:oxygen, the current knowledge regarding the specific binding site of oxygen in flavoenzymes are still under debate. A specific oxygen binding site in flavoenzymes is

not well defined although a hydrophobic tunnel that may be relevant for oxygen diffusion is found in cholesterol oxidase [28]. Based on structures of flavin-dependent oxidases and monooxygenases and molecular dynamics simulations, the oxygen approach to the flavin C4a-position is proposed to be "edge-on" for the oxidases and "face-on" for the monooxygenases [29, 30]. We could not identify any clear oxygen binding site in the active site of *Mp*GlpO– and the approach for oxygen diffusion in *Mp*GlpO is via the "edge-on" approach [23].

In conclusion, our results indicate that the kinetic mechanism of His_6-*Mp*GlpO is a ping-pong type in which DHAP leaves before the oxidative half-reaction with oxygen. H_2O_2 release is likely the rate-limiting step for the overall turnover. The rapid kinetics of both half-reactions showed biphasic kinetics which is due to a mixture of fast and slow reacting enzyme species. The enzyme can catalyze the reverse reaction of reduced His_6-*Mp*GlpO and DHAP. It can also use GAP as a substrate, implying its involvement in the glycolysis pathway in addition to the pathways of glycerol and lipid metabolism. Thus, the contributions from this work can serve as the groundwork for future development of inhibitors against GlpO for the prevention of *M. pneumonia* infection.

Experimental Procedures

Chemicals and reagents

Flavin adenine dinucleotide disodium salt hydrate (FAD), horseradish peroxidase, type I (HRP), 2,2'-azino-bis(3-ethylbenzothiazoline-6-sulfonic acid) diammonium salt (ABTS), L-α-glycerophosphatebis(cyclohexylammonium) salt (Glp), DL-glyceraldehyde 3-phosphate solution (GAP), and dihydroxyacetone phosphate dilithium salt (DHAP)

were purchased from Sigma-Aldrich (St. Louis, MO, USA).Isopropyl β-D-1-thiogalactopyranoside (IPTG) was purchased from Fermentas Life Sciences (Glen Burnie, MD, USA). All chromatographic media were purchased from GE Healthcare Biosciences (Uppsala, Sweden).

The concentrations of the following compounds were determined using the known extinction coefficients at pH 7.0: ε_{450} = 11.3 $mM^{-1}cm^{-1}$ for FAD, ε_{403} = 100 $mM^{-1}cm^{-1}$ for HRP. The concentrations of Glp in the stock solutions were calculated based on the reducing equivalents in the reduction of the purified recombinant His_6-*Mp*GlpO. A solution (1 mL) of His_6-*Mp*GlpO was prepared, made anaerobic and the concentration was determined using the molar absorption coefficient at 448 nm of 12.4 $mM^{-1}cm^{-1}$. A solution of Glp was then titrated into the enzyme solution under anaerobic conditions inside an anaerobic glovebox (<5 ppm oxygen; Belle Technology, UK). The absorbance change at 448 nm (ΔA_{448}) of the enzyme before and after the reduction was used for calculating the concentration of the enzyme that was reduced by Glp which is equivalent to the amount of Glp added. The molar equivalent of Glp was used for calculating the concentration of the stock solution.

Spectroscopic studies

UV-Visible absorbance spectra were recorded with a diode-array spectrophotometer (Hewlett Packard, Palo Alto, CA, USA), a Shimadzu 2501PC (SHIMADZU 2501PC, Shimadzu Corp., Kyoto, Japan)or a Cary 300Bio (Varian Inc., Palo Alto, CA, USA) spectrophotometer. Steady-state and pre-steady-state kinetics studies were carried out using a stopped-flow spectrophotometer (TGK Scientific

instruments, model SF-61DX2 or SF-61SX) in both single and double-mixing modes. All instruments were equipped with thermostatic cell compartments.

Enzyme assay

The activity of His_6-*Mp*GlpO was measured by monitoring the amount of H_2O_2 formed using the HRP coupled assay [31, 32]. HRP uses the H_2O_2 generated from the His_6-*Mp*GlpO-catalyzed reaction to oxidize reduced ABTS to generate oxidized ABTS, which is dark green with a λ_{max} at 420 nm and a molar absorption coefficient of 42.3 $mM^{-1}cm^{-1}$ (per one mole of Glp consumed). The assay mixture in 50 mM sodium phosphate buffer, pH 7.0 typically contained 15 mM Glp, 1 mM ABTS, and 600 nM HRP. The enzyme activity was measured by monitoring the increase in absorbance at 420 nm which is due to ABTS oxidation. One unit of His_6-*Mp*GlpO activity was defined as the amount of enzyme required to oxidize one micromole of Glp per min.

Expression and purification of His_6-MpGlpO

A single colony of *E. coli* BL21(DE3) harboring the His_6-*Mp*GlpO expression plasmid, pET28a-*mpglpo*, was inoculated into 100 mL of Terrific Broth (in a 500-mL Erlenmeyer flask) containing 30 μg/mL kanamycin, and cultured overnight in a shaking incubator at 37 °C. An overnight culture with a final ratio of 1% (v/v) was inoculated into 6 × 800 mL of Terrific Broth containing 30 μg/mL kanamycin. A large-scale culture was grown at 37 °C until the absorbance at 600 nm reached ~1. The culture was then cooled down to 25 °C and induced by the addition of IPTG at a final concentration of 1 mM and

maintained at this temperature for ~12 h. Cells were harvested by centrifugation and stored at -80 ^{o}C until used.

Unless otherwise indicated, purification of the His_6-*Mp*GlpO was conducted at 4 ^{o}C. Frozen cell paste was thawed and resuspended in 50 mM sodium phosphate buffer, pH 7.0 containing 200 mM NaCl, 10% (v/v) glycerol, 10 mM imidazole, 1 mM DTT, 0.5 mM EDTA, and 100 μM PMSF. Cells were lysed by ultrasonication (Sonic Vibra_cell™ model VCX750). The disrupted cell suspension was then centrifuged at 35,000 ×g for 1 h. The supernatant was additionally clarified by ultracentrifugation at 100,000 ×g for 1.5 h and then loaded onto a Ni-Sepharose (GE Healthcare) column (2.5 × 7.0 cm; volume ~34 mL) pre-equilibrated with 300 mL of 50 mM sodium phosphate buffer, pH 7.0 containing 200 mM NaCl, 10% (v/v) glycerol and 10 mM imidazole. The column was then washed with the same buffer for 300 mL and subsequently eluted with 400 mL of a linear gradient of 10-500 mM imidazole in 50 mM sodium phosphate buffer, pH 7.0 containing 200 mMNaCl, and 10% (v/v) glycerol. Fractions containing the His_6-*Mp*GlpO were identified by measuring the absorbance at 448 nm, pooled, and concentrated using a stirred cell apparatus (Amicon® 8050) equipped with a Millipore membrane YM-10 (10 kDa cut-off). Free FAD was added during the concentration process to make sure that the enzyme fully bound to FAD. An enzyme solution of ~100 mL was thentransferred into a dialysis bag (Sigma-Aldrich) and dialyzed against 4 L of 50 mM sodium phosphate buffer, pH 7.0 containing 0.5 mM EDTA for overnight. The dialyzed sample was loaded onto an SP-Sepharose (GE Healthcare) column (2.5 × 13.0 cm; volume ~64 mL) pre-equilibrated with 700 mL of 50 mM sodium phosphate buffer, pH 7.0 containing 0.5 mM EDTA and 150 mM NaCl. The column was washed with 700 mL of the same buffer and

then eluted with 800 mL of a linear gradient of 150-800 mMNaCl in 50 mM sodium phosphate buffer, pH 7.0 containing 0.5 mM EDTA. Fractions containing the enzyme were identified, pooled and concentrated as described above. A solution of ~6-8 mL of the purified enzyme was desalted and exchanged into 100 mM Tris-H_2SO_4, pH 7.0 containing 0.5 mM EDTA using a Sephadex G-25 (GE Healthcare) column (1.5 × 60.0 cm; volume ~106 mL). The desalted enzyme was then aliquoted in 500 μL portions in each microcentrifuge tube and kept at -80 ^{o}C until used. The purity of the enzyme was estimated by 12% (w/v) sodium dodecyl sulfate-polyacrylamide gel electrophoresis. The protein amount was determined using a Bradford method and BSA as a standard protein.

Determination of molar extinction coefficients of His_6-MpGlpO-bound FAD

The methods for the determination of the molar absorption coefficients of His_6-*Mp*GlpO-bound FAD were slightly modified from a general procedure [33]. The frozen purified enzyme was quickly thawed and exchanged into 50 mM sodium phosphate buffer, pH 7.0 using a PD-10 column (GE Healthcare). The holoenzyme solution (900 μL) was added 100 μL of 20% (w/v) SDS solution to give a final absorbance value of the enzyme of ~0.25 and a final SDS concentration of 2% (w/v). The same buffer (100 μM) was added to another aliquot of holoenzyme (900 μL). The absorption spectra of both solutions were recorded and compared. The concentration of released FAD was calculated based on the FAD molar extinction coefficient of 11.3 $mM^{-1}cm^{-1}$at 450 nm. For the holoenzyme, the molar extinction coefficient at 448 nm (λ_{max}) can be determined according to Eqn1, on the basis that the apoenzyme binds FAD with a ratio of 1:1 mol. A_{enzyme} represents enzyme absorbance while A_{FAD} represents FAD absorbance.

$$\varepsilon_{enzyme} = \frac{A_{enzyme}}{A_{FAD}} x \varepsilon_{FAD} \quad (1)$$

Steady-State Kinetics

Two-substrate steady-state kinetics of the His_6-*Mp*GlpO was carried out in 50 mM sodium phosphate buffer, pH 7.0 at 4°C using an ABTS coupled-enzyme assay as previously described [34] and monitored by the Hi-Tech Scientific model SF-61DX stopped-flow spectrophotometer in single-mixing mode. The optical pathlength of the observation cell was 1 cm. A mixture of 5.16 nM His_6-*Mp*GlpO, 600 nM HRP, and 1 mM ABTS was mixed against solutions of various concentrations of Glp (4, 8, 16, and 32 mM) and oxygen (0.13, 0.26, 0.44, 0.65, 1.16 mM). The reaction progress was followed by monitoring the increase of absorbance at 420 nm at which the oxidized ABTS absorbs with the molar extinction coefficient of 42.3 $mM^{-1}cm^{-1}$ (per one mole of Glp consumed) [31, 32]. Kinetic traces obtained from each reaction (performed in triplicate) were calculated their initial rates using Program A (developed by Chun-Jen Chiu, Rong Chang, Joel Dinverno, and David P. Ballou at the University of Michigan, Ann Arbor, MI). The initial rates were then analyzed for steady-state kinetic parameters of a bi-substrate enzyme reaction according to either a double-reciprocal plot of a ping-pong mechanism (Eqn 2) [35] or a direct plot (Eqn 3) using the EnzFitter program (BIOSOFT, Cambridge, UK).

Apparent steady-state kinetics of the His_6-*Mp*GlpO reaction was performed in air-saturated (oxygen concentration of ~0.26 mM) 50 mM sodium phosphate buffer, pH 7.0 at 25 °C at various concentrations of DL-glyceraldehyde 3-phosphate (GAP) (0.025-6.4 mM) using the coupling assay with horseradish peroxidase-coupled assay. The reactions

were monitored at 420 nm as described above. The initial rates were calculated and then plotted *versus* GAP concentration. Apparent kinetic parameters were calculated using Marquardt-Lavenberg algorithms in the KaleidaGraph program version 4.0 and compared to the reaction using various concentrations of Glp (0.1-51.2 mM) under the same conditions.

$$\frac{e}{v} = \phi_0 + \frac{\phi_A}{[A]} + \frac{\phi_B}{[B]} \quad (2)$$

$$v = \frac{V[A][B]}{K_B[A] + K_A[B] + [A][B]} \quad (3)$$

Binding of the oxidized His$_6$-MpGlpO with products

A solution (1 mL) of the oxidized enzyme (A_{448} ~0.3; 24 μM) in 50 mM sodium phosphate buffer, pH 7.0 was placed in both sample and reference cells. Then, a baseline was recorded. Various concentrations of H_2O_2 (0.16-371 mM) or DHAP (0.005-30 mM) were added into the enzyme solution in the sample cell while an equal volume of buffer was added into the reference cell. An absorption spectrum was recorded after each titration using a double-beam spectrophotometer. The changes in absorbance were plotted against the concentrations of each product. Dissociation constants for the binding of products to the oxidized enzyme were determined and analyzed according to the method previously described [36] and Eqn 4, where ΔA represents the absorbance change, ΔA_{max} is the maximum absorbance change, $[L]_{free}$ is a concentration of free ligand, and K_d is a dissociation constant for enzyme-ligand complex. The analysis was done using Marquardt-Lavenberg algorithms in the KaleidaGraph program version 4.0. Similar

protocol and data analysis were also applied for spectrophotometric titration of the FAD solution (A_{450} ~0.3) with H_2O_2 using a similar range of concentrations. For the binding of enzyme with other substrate analogues –glycerol, L-lactate, and D,L-malate– the reactions and analysis were performed and carried out as mentioned above, except that the concentrations of glycerol, L-lactate, and D,L-malate used were varied from 0.16-371 mM.

$$\frac{\Delta A}{\Delta A_{max}} = \frac{[L]_{free}}{K_d + [L]_{free}} \quad (4)$$

Binding and reaction of the reduced His_6-MpGlpO with DHAP

A solution (1 mL) of the oxidized enzyme (A_{448} ~0.3; 24 μM) in 50 mM sodium phosphate buffer, pH 7.0 was placed in an anaerobic glove box in which the oxygen concentration was less than 5 ppm (Belle Technology, UK) to remove trace amounts of oxygen and then reduced by a stoichiometric concentration of dithionite under anaerobic conditions. Various concentrations of DHAP (0.69-4,308 μM) were subsequently added to the reduced enzyme. All concentrations reported above are final concentrations after mixing. A spectrum after each titration was recorded by a Gene Quant 1300 spectrophotometer (GE Healthcare, UK) residing in the anaerobic glove box. The spectrum of reduced enzyme was subtracted from all the spectra obtained from each titration to give the change in absorbance (ΔA). Analysis was done according to the method previously described [36].

As the results indicate that the reverse reaction of the reduced enzyme and DHAP can occur, the kinetics of the enzyme re-oxidation by DHAP was further explored using

stopped-flow spectrophotometry at 4 °C. The reduced enzyme (16 μM) in 50 mM sodium phosphate buffer, pH 7.0 was mixed with various concentrations of DHAP (0.1-12.8 mM) under anaerobic conditions using a single-mixing mode of a stopped-flow apparatus. All concentrations shown above are given as final concentrations after mixing. The reactions were monitored at 448 nm and the final spectra after the reaction were recorded. Kinetic traces were analyzed by Program A and the observed rate constants (k_{obs}) were plotted *versus* DHAP concentrations. The plots were analyzed according to Eqn 5, where k_1 is a bimolecular rate constant for the reduced enzyme re-oxidation.

$$k_{obs} = k_1 \cdot [\mathrm{DHAP}] \qquad (5)$$

Measurement of the standard reduction potential of His$_6$-MpGlpO

Standard reduction potential of His$_6$-*Mp*GlpO was measured in 50 mM sodium phosphate buffer, pH 7.0 at 25 °C by Massey's method using the xanthine/xanthine oxidase reduction system with benzyl viologen as an electron mediator [37]. The reference dye used for measuring the standard reduction potential of His$_6$-*Mp*GlpO was cresyl violet which has a standard reduction potential (E^0_m) value of -166 mV [38]. A solution mixture of dye (A_{519} ~0.3) and the oxidized enzyme (A_{448} ~0.3; 24 μM), benzyl viologen (5.3 μM), and xanthine (0.5 mM) in 50 mM sodium phosphate buffer, pH 7.0 was placed in an anaerobic cuvette and made anaerobic by purging with oxygen-free nitrogen for 10-12 cycles to evacuate trace amounts of oxygen. The spectrum of the oxidized species was then recorded. The anaerobic solution was then tipped into xanthine oxidase (10 nM) from the cuvette sidearm and the spectral changes were recorded. All

concentrations shown above are as after mixing. The enzyme and dye were slowly reduced (>8 hr) so that the reduction process was under equilibrium. The reduction potentials of enzyme (E_e) and dye (E_d) were determined according to Eqns 6 and 7, respectively, in which E_{red} and E_{ox} are the concentrations of the reduced and oxidized enzyme, respectively, D_{red} and D_{ox} are the concentrations of the reduced and oxidized dye, respectively, E_e^0 and E_d^0 are the standard reduction potential values of enzyme and dye, respectively, and n_e and n_d are the numbers of electrons involved in the reduction process. At equilibrium, the value of E_e is equivalent to E_d and Eqns 6 and 7 can be rearranged to Eqn 8 which can be used for determining the E_e^0 value. After the complete reduction, the absorbance at 407 nm (isobestic point of a reference dye) and 540 nm were used for calculating the concentrations of the oxidized enzyme (E_{ox}) and the reduced dye (D_{red}) during the reduction process, respectively. The concentrations of reduced and oxidized enzyme (E_{red}) and dye (D_{ox}) at different points of the reduction process were analyzed with Eqn 8 to determine the standard reduction potential value (E_e^0) of the enzyme.

$$E_e = E_e^0 - \frac{0.0592}{n_e}\log(E_{red}/E_{ox}) \quad (6)$$

$$E_d = E_d^0 - \frac{0.0592}{n_d}\log(D_{red}/D_{ox}) \quad (7)$$

$$\log(E_{red}/E_{ox}) = \frac{n_e(E_e^0 - E_d^0)}{0.0592} + (n_e/n_d)\log(D_{red}/D_{ox}) \quad (8)$$

Reductive half-reaction of His$_6$-MpGlpO

A solution of anaerobic oxidized enzyme (~28μM; A_{448} ~0.35) in 50 mM sodium phosphate buffer, pH 7.0 containing 0.5 mM EDTA, and 1 mM DTT was mixed with various concentrations of Glp (0.2-51.2mM) under anaerobic conditions using the stopped-flow spectrophotometer at 4 ^{o}C. All concentrations shown are as after mixing. Kinetics of the enzyme reduction was monitored by the absorbance change at 448 nm. The kinetic traces were analyzed by Program A to obtain observed rate constants from each exponential phase. The observed rate constants obtained were plotted *versus* Glp concentrations. The results were then analyzed with Eqn9, where k_{obs} is the observed rate constants, k_{max} is the rate constant for flavin reduction (k_{red}), S is Glp concentration, and K_d is the dissociation constant for substrate binding. The analysis was carried out using Marquardt-Lavenberg algorithms in KaleidaGraph program version 4.0.

$$k_{obs} = \frac{k_{max} \cdot [S]}{K_d + [S]} \qquad (9)$$

Oxidative half-reaction of His$_6$-MpGlpO

The anaerobically oxidized enzyme (~28μM; A_{448} ~0.35) in 50 mM sodium phosphate buffer, pH 7.0 containing 0.5 mM EDTA, and 1 mM DTT was titrated stoichiometrically with Glp to yield the reduced enzyme. The reduced enzyme was then mixed with various concentrations of oxygen (0.13, 0.32, 0.61, 1.03mM) using a stopped-flow spectrophotometer at 4^{o}C. All concentrations shown are as after mixing. The kinetics of enzyme oxidation was monitored by absorbance at 448 nm. The kinetic traces were analyzed by Program A to obtain the observed rate constants. The plots of k_{obs} as a

function of oxygen concentrations were analyzed using Eqn 9, in which k_{max} is the rate constant for flavin oxidation (k_{ox}), S is oxygen concentration, and K_d is the dissociation constant for oxygen binding. The analysis was carried out using Marquardt-Lavenberg algorithms in KaleidaGraph program version 4.0.

Reactions of the Glp-reduced His$_6$-MpGlpO with O_2 in a double-mixing mode

Double-mixing stopped-flow experiments were done to evaluate whether the presence of DHAP can affect the oxygen reaction. An anaerobic solution of the oxidized His$_6$-*Mp*GlpO (91 μM) in Syringe A was mixed first with Glp (91 μM) in Syringe B. The reactions were aged for 100 s to allow the enzyme reduction to proceed. The solution from the first mixing was later mixed with various concentrations of oxygen (0.26, 0.61, 1.03, 2.06 mM) in 50 mM sodium phosphate buffer, pH 7.0 in the second mix. The reactions were monitored at 448 nm with a double-mixing mode stopped-flow spectrophotometer (Hi-Tech Scientific Model SF-61DX). All concentrations shown are initial concentrations before mixing. The kinetic traces were analyzed by Program A and the k_{obs} values of individual phases were plotted *versus* oxygen concentration. The plots were analyzed according to Eqn 9 using Marquardt-Lavenberg algorithms in KaleidaGraph program version 4.0. Results of this reaction were compared to the results of single-mixing mode oxidative half-reaction experiments previously described.

Reactions of the dithionite-reduced His$_6$-MpGlpO with O_2 in the presence of DHAP

An anaerobic solution of the dithionite-reduced His$_6$-*Mp*GlpO (91 μM) in Syringe A was mixed first with DHAP (136.5 μM) in Syringe B at various age times (10, 20, 100,

and 200 s). The solution mixture was then mixed with oxygen (0.26 mM) in 50 mM sodium phosphate buffer, pH 7.0 in the second mix. The reactions were monitored at 448 nm by double-mixing mode stopped-flow experiments. All concentrations shown are initial concentrations before mixing. The kinetic traces were analyzed by Program A and the kinetics results at various age times were compared to the results obtained from the oxidative half-reaction in the absence of DHAP.

Acknowledgements

This work was supported by grants from The Thailand Research Fund MRG5580066 (to SM) and RTA5680001 (to PC), the Faculty of Science, Burapha University (to SM) and the Faculty of Science, Mahidol University (to PC). We would like to thank Dr. Ruchanok Tinikul (MahidolUniversity Nakhonsawan Campus) for her help with the molecular biology work. We are grateful for Professor Dr. David P. Ballou (University of Michigan, Ann Arbor) for helpful discussion.

References

1. Koditschek LK &Umbreit WW (1969) α-Glycerophosphate oxidase in *Streptococcus faecium*F24.*J Bacteriol***98**, 1063-1068.

2. Esders TW &Michrina CA (1979) Purification and properties of α-glycerophosphate oxidase from *Streptococcus faecium* ATCC 12755. *J BiolChem***254**, 2710-2715.

3. Claiborne A (1986) Studies on the structure and mechanism of *Streptococcus faecium* L-α-glycerophosphate oxidase. *J BiolChem***261**, 14398-14407.

4. Halbedel S, Hames C &Stulke J (2007) Regulation of carbon metabolism in the mollicutes and its relation to virulence. *JMolMicrobiolBiotechnol***12**, 147-154.

5. Hames C, Halbedel S, Hoppert M, Frey J &Stulke J (2009) Glycerol metabolism is important for cytotoxicity of *Mycoplasma pneumoniae*. *J Bacteriol***191**, 747-753.

6. Veal EA, Day AM & Morgan BA (2007) Hydrogen peroxide sensing and signaling. *Mol Cell***26**, 1-14.

7. Almagor M, Kahane I &Yatziv S (1984) Role of superoxide anion in host cell injury induced by *Mycoplasma pneumoniae* infection: a study in normal and trisomy 21 cells. *J Clin Invest***73**, 842-847.

8. Pilo P, Vilei EM, Peterhans E, Bonvin-Klotz L, Stoffel MH, Dobbelaere D & Frey J (2005) A metabolism enzyme as a primary virulence factor of *Mycoplasma mycoides* subsp. *mycoides* small colony. *J Bacteriol***187**, 6824-6831.

9. Waites KB &Talkington DF (2004) *Mycoplasma pneumoniae* and its role as a human pathogen. *ClinMicrobiol Rev***17**, 696-728.

10.Fairlamb AH &Bowman IBR (1977) *Trypanosomabrucei*: suramin and other trypanocidal compounds' effect on *sn*-glycerol-3-phosphate oxidase. *ExpParasitol***43**, 353-361.

11. Opperdoes FR, Borst P &Fonck K (1976) The potential use of inhibitors of glycerol-3-phosphate oxidase for chemotherapy of African trypanosomiasis. *FEBS Lett***62**, 169-172.

12. Fairlamb AH & Bowman IBR (1977) The isolation and characterisation of particulate *sn*-glycerol-3-phosphate oxidase from *Trypanosomabrucei*. *Int J Biochem***8**, 659-668.

13. Fairlamb AH & Bowman IBR (1977) Inhibitor studies on particulate sn-glycerol-3-phosphate oxidase from *Trypanosomabrucei*. *Int J Biochem***8**, 669-675.

14. Grady RW, Bienen EJ & Clarkson AB (1986) Esters of 3,4-dihydroxybenzoic acid, highly effective inhibitors of the *sn*-glycerol-3-phosphate oxidase of *Trypanosomabruceibrucei*. *MolBiochemParasitol***21**, 55-63.

15. Parsonage D, Luba J, Mallett TC & Claiborne A (1998) The soluble α-glycerophosphate oxidase from *Enterococcus casseliflavus*. *J BiolChem***273**, 23812-23822.

16. Charrier V, Luba J, Parsonage D & Claiborne A (2000) Limited proteolysis as a structural probe of the soluble α-glycerophosphate oxidase from *Streptococcus* sp. *Biochemistry* **39**, 5035-5044.

17. Finnerty CM, Charrier V, Claiborne A &Karplus PA (2002) Crystallization and preliminary crystallographic analysis of the soluble α-glycerophosphate oxidase from *Streptococcus* sp. *ActaCrystallogr D BiolCrystallogr***D58**, 165-166.

18. Colussi T, Parsonage D, Boles W, Matsuoka T, Mallett TC, Karplus PA & Claiborne A (2008) Structure of α-glycerophosphate oxidase from *Streptococcus* sp.: a template for the mitochondrial α-glycerophosphate dehydrogenase. *Biochemistry***47**, 965-977.

19.Fersht A (1999) Measurement and magnitude of individualrate constants. In*Structure and Mechanism in Protein Science: A Guide to Enzyme Catalysis and Folding*, pp 132−167. W.H. Freeman & Co., NewYork, NY.

20. Dawson RMC, Elliot DC, Elliot WH & Jones KM (1986) *Data for biochemical research*, 3rd edn. Oxford University Press, New York, NY.

21. Dewanti AR &Mitra B (2003) A transient intermediate in the reaction catalyzed by (*S*)-mandelate dehydrogenase from *Pseudomonas putida*. *Biochemistry***42**, 12893-12901.

22. Vilei EM & Frey J (2001) Genetic and biochemical characterization of glycerol uptake in *Mycoplasma mycoides* subsp. *mycoides* SC: its impact on H_2O_2 production and virulence. *ClinDiagn Lab Immunol***8**, 85-92.

23. Elkhal CK, Kean K, Parsonage D, Maenpuen S, Chaiyen P, Claiborne A & Karplus PA (2015) Structure and proposed mechanism of α-glycerophosphate oxidase from *Mycoplasma pneumoniae*. *Article in Revision*.

24. Sucharitakul J, Prongjit M, Haltrich D & Chaiyen P (2008) Detection of a C4a-hydroperoxyflavin intermediate in the reaction of a flavoprotein oxidase. *Biochemistry***47**, 8485-8490.

25. Wongnate T, Surawatanawong P, Visitsatthawong S, Sucharitakul J, Scrutton NS & Chaiyen P (2014) Proton-coupled electron transfer and adduct configuration are important for C4a-hydroperoxyflavin formation and stabilization in a flavoenzyme. *J Am ChemSoc***136**, 241-253.

26. Ruangchan N, Tongsook C, Sucharitakul J & Chaiyen P (2011) pH-dependent studies reveal an efficient hydroxylation mechanism of the oxygenase component of *p*-hydroxyphenylacetate 3-hydroxylase. *J BiolChem***286**, 223-233.

27. Thotsaporn K, Chenprakhon P, Sucharitakul J, Mattevi A&Chaiyen P (2011) Stabilization of C4a-hydroperoxyflavin in a two-component flavin-dependent monooxygenase is achieved through interactions at flavin N5 and C4a atoms.*J BiolChem***286**, 28170-80.

28. Chen L, Lyubimov AY, Brammer L, Vrielink A & Sampson NS (2008) The binding and release of oxygen and hydrogen peroxide are directed by a hydrophobic tunnel in cholesterol oxidase. *Biochemistry* **47**, 5368-5377.

29. Baron R, Riley C, Chenprakhon P, Thotsaporn K, Winter RT, Alfieri A, Forneris F, van Berkel WJ, Chaiyen P, Fraaije MW, Mattevi A &McCammon JA (2009) Multiple pathways guide oxygen diffusion into flavoenzyme active sites. *ProcNatlAcadSci USA* **106**, 10603-10608.

30. Chaiyen P, Fraaije MW &Mattevi A (2012) The enigmatic reaction of flavins with oxygen. *Trends BiochemSci***37**, 373-380.

31. Prongjit M, Sucharitakul J, Wongnate T, Haltrich D & Chaiyen P (2009) Kinetic mechanism of pyranose 2-oxidase from *Trametes multicolor*. *Biochemistry***48**, 4170-4180.

32. Pitsawong W, Sucharitakul J, Prongjit M, Tan TC, Spadiut O, Haltrich D, Divne C &Chaiyen P (2010) A conserved active-site threonine is important for both sugar and flavin oxidations of pyranose 2-oxidase. *J BiolChem***285**, 9697-9705.

33. Macheroux P (1999) UV-visible spectroscopy as a tool to study flavoproteins, In *Flavoprotein Protocols*,(Chapman, S.K., & Reid, G.A., eds.), pp. 1-7, Humana Press. Totowa, NJ.

34. Daneel HJ, Rossner E, Zeeck A &Giffhorn F (1993) Purification and characterization of a pyranose oxidase from the basidiomycete*Peniophoragigantea* and chemical analyses of its reaction products. *Eur J Biochem***214**, 795-802.

35. Dalziel K (1957) Initial steady-state velocities in the evaluation of enzyme-coenzyme-substrate reaction mechanism. *ActaChemScand***11**, 1706-1723.

36. Chenprakhon P, Sucharitakul J, Panijpan B & Chaiyen P (2010) Measuring binding affinity of protein-ligand interaction using spectrophotometry: binding of neutral red to riboflavin-binding protein. *J Chem Ed***87**, 829-831.

37. Massey V (1991) A simple method for the determination of redox potentials, In *Flavins and Flavoproteins* (Curti, B., Rochi, S., &Zanetti, G., eds.) pp. 59-66, Water DeGruyter&Co., Berlin, Germany.

38. Clark WM (1960) Compilations of data in *oxidation-reduction potentials of organic systems*. pp. 410, Wavery Press, Inc., Baltimore.

Table 1: Purification table of the recombinant His_6-*Mp*GlpO

	Volume (mL)	Total Activity (U)	Total Protein (mg)	Specific Activity (U/mg)	Yield (%)
Crude extract	180	13,968	10,746	1.3	100
Ni-Sepharose	150	2,775	244.5	11.4	20
SP-Sepharose	9	1,638	163.8	10	12

*The data in this table were from the purification of 83 g cell paste (8.8 liters culture).

Table 2: Thermodynamics and kinetic parameters involved in the His_6-*Mp*GlpO reaction

Parameters	Constants
Fast reacting enzyme	
k_1, formation of E_{ox}:Glp complex	83.3 $M^{-1}s^{-1}$
k_2, Glp release	6 s^{-1}
k_3, enzyme reduction	199 ± 34 s^{-1}
k_4, reverse reaction of E_{red} and DHAP	56.5 $M^{-1}s^{-1}$
k_5, k_6, k_{10}	ND
k_7, re-oxidation of reduced enzyme	627 ± 81 s^{-1}
k_9, H_2O_2 release	4.2 ± 0.1 s^{-1}
K_{d1}, dissociation constant for E_{ox}:Glp complex	72 ± 18 mM
K_{d2}, dissociation constant for E_{red}:O_2 complex	1.3 ± 0.2 mM
K_{d3}, dissociation constant for E_{red}:H_2O_2 complex	0.4 ± 0.2 mM
Slow reacting enzyme	
k_1', k_2', k_4', k_5', k_6'	ND
k_3', enzyme reduction	2.08 ± 0.01 s^{-1}
k_7', re-oxidation of reduced enzyme	85 ± 11 s^{-1}
$K_{d1'}$, dissociation constant of E^*_{ox}:Glp complex	1.38 ± 0.02 mM
$K_{d2'}$, dissociation constant of E^*_{red}:O_2 complex	0.5 ± 0.1 mM
k_{obs} for interconversion of fast and slow reacting enzymes	
$k_f + k_r$	> 6 s^{-1}, <16 s^{-1}

ND = Not determined

Figure legends

Fig. 1. Absorption and reduction properties of His_6-*Mp*GlpO. (A) Absorption spectra of the enzyme-bound FAD (solid line) and the released FAD upon denaturation by 2% (w/v) SDS (dashed line) are overlaid. The molar absorption coefficient of His_6-*Mp*GlpO was determined as12.40 ± 0.03 $mM^{-1}cm^{-1}$. (B) Standard reduction potential measurement of His_6-*Mp*GlpO at 25 °C by Massey's method using benzyl viologen-mediated xanthine/xanthine oxidase reaction system. The standard reduction potential value (E_e^0) of the enzyme calculated from the y-intercept of the plot of $\log(E_{red}/E_{ox})$ *versus* $\log(D_{red}/D_{ox})$ is -167 ± 1 mV (Inset of B).

Fig. 2. Two-substrate steady-state kinetics of the His_6-*Mp*GlpO reaction at 4 °C. The assay reactions were monitored by the HRP coupled-assay using a stopped-flow spectrophotometer. (A) Initial rates obtained from various concentrations of Glp and O_2 were measured and plotted as a double-reciprocal plot of e/v_o *versus* 1/[Glp] at various concentration of O_2 (0.13-1.16 mM from upper to lower lines) or (B) *versus* $1/[O_2]$ at various concentrations of Glp (4-32 mM from upper to lower lines). Both double-reciprocal plots in A and B show a parallel-line pattern, indicating that His_6-*Mp*GlpO uses a ping-pong mechanism.

Fig. 3. Reductive half-reaction of His_6-*Mp*GlpO at 4 °C. A solution of the oxidized enzyme (~28 μM) was mixed with various concentrations of Glp (0.4-51.2 mM from right to left traces) under anaerobic conditions using a single-mixing mode of the stopped-flow apparatus. (A) The reaction kinetics was monitored by measuring the

absorbance change at 448 nm. Kinetic analyses indicate that the enzyme reduction is biphasic. (B-C) Plots of k_{obs} values obtained from both phases *versus* Glp concentrations are hyperbolic with limiting reduction rate constant values of 199 ± 34 (B) and 2.08 ± 0.01 s^{-1} for the fast and slow reacting enzyme, respectively. The data suggest that the enzyme reduction involves a two-step process in which one population reacts faster than another. (D) Apparent steady-state kinetics of His_6-*Mp*GlpO using GAP and Glp as substrates at 25 ^oC. Initial rates obtained from the reaction using GAP (0.025-6.4 mM) were directly plotted *versus* GAP concentrations while those obtained from the reaction using Glp (0.1-51.2 mM) as a substrate are shown in the inset. The results indicated that the k_{cat} and k_{cat}/K_m of the reaction using Glp as a substrate are 100- and 15-fold greater than those of GAP, respectively. (E) Proposed kinetic scheme for the reductive half-reaction of His_6-*Mp*GlpO.

Fig. 4. Oxidative half-reaction of the reduced His_6-*Mp*GlpO at 4 ^oC. An anaerobic solution of the reduced enzyme was mixed with various concentrations (0.13-1.03 mM from lower to upper traces) of oxygenated buffer using a single-mixing mode of stopped-flow apparatus. (A) The reaction kinetics was monitored by the absorbance change at 448 nm. (B-C) Kinetic analyses indicated that the kinetics of the reaction of the reduced enzyme with O_2 is biphasic and the plots of k_{obs} values of both phases *versus* O_2 concentrations are hyperbolic. The ratio of amplitude change for both phases is 70:30 throughout all oxygen concentrations used. The limiting rate constant values for the reduced enzyme re-oxidation for the fast and slow reacting enzyme are 627 ± 81 and 85 ± 11 s^{-1}, respectively. (D) Proposed kinetic scheme for the oxidative half-reaction of His_6-

*Mp*GlpO.

Fig. 5. Double-mixing stopped-flow experiments of reduced His_6-*Mp*GlpO reacting with oxygen at 4 ^{o}C. A solution of the oxidized enzyme (91 μM before mixing) was added to Glp (91 μM before mixing) in the first mix and then mixed with various concentrations of O_2 (0.26-2.06 mM before mixing; from lower to upper traces) in the second mix. (A) The reaction kinetics was monitored by changes in the absorbance at 448 nm. Kinetic analyses indicated that all reaction traces display biphasic kinetics and amplitude changes that are similar to those obtained from the oxidative half-reaction performed in the single-mixing mode (Fig. 4A). (B-C) The plots of k_{obs} values *versus* oxygen concentrations are hyperbolic with the rate constant (k_{ox}) values for enzyme re-oxidation of 524 ± 34 and 107 ± 5 s^{-1} that are similar to those obtained from the results in Figs. 4B and 4C. The similarity in these kinetic behaviors suggests that DHAP is quickly released after its formation. (D) In another experiment, a solution of the dithionite-reduced enzyme (91 μM before mixing) was added to DHAP (136.5 μM before mixing) for various age times (10, 20, 100, and 200 s) in the first mix and then mixed with the oxygenated buffer (O_2 = 0.26 mM before mixing) in the second mix. All kinetics traces were similar and also similar to the results in (A) and in Fig. 4. Altogether, complex of reduced enzyme and DHAP could not be detected, implying that the DHAP release is fast during the catalytic turnover of His_6-*Mp*GlpO.

Fig. 6. The reaction of the reduced His_6-*Mp*GlpO with DHAP. (A) A solution of the reduced enzyme (24 μM) was mixed with various concentrations of DHAP (0.69-4,308

μM (from lower to upper spectra). The binding signal was measured by spectrophotometry at 25 ^{o}C. Difference spectra showed that binding of DHAP to the reduced enzyme caused enzyme re-oxidation as indicated by the increase of absorbance at 448 nm. (B) Pseudo-first order kinetics for the reaction of the reduced enzyme and various concentrations of DHAP (0.2-12.8 mM from lower to upper traces) was monitored under anaerobic conditions using a single-mixing mode stopped-flow spectrophotometer at 4 ^{o}C. The kinetic traces at 448 nm were recorded. (C-D) Kinetic analysis indicated that the reaction is biphasic and the k_{obs} values obtained from the first phase are constant (6 s^{-1}) while those of the second phase are linearly dependent on DHAP concentrations with a bimolecular rate constant of 56.5 $M^{-1}s^{-1}$. (E) Proposed scheme for the reverse reaction of reduced His_6-*Mp*GlpO and DHAP.

Fig. 7. Proposed overall catalytic reaction of His_6-*Mp*GlpO. Two enzyme populations (fast and slow reacting species) react with substrates in both half-reactions. The reverse flavin oxidation is shown as the red arrows (see text for details). Thermodynamics and kinetics parameters are presented in Table 2.

Figures

Fig. 1

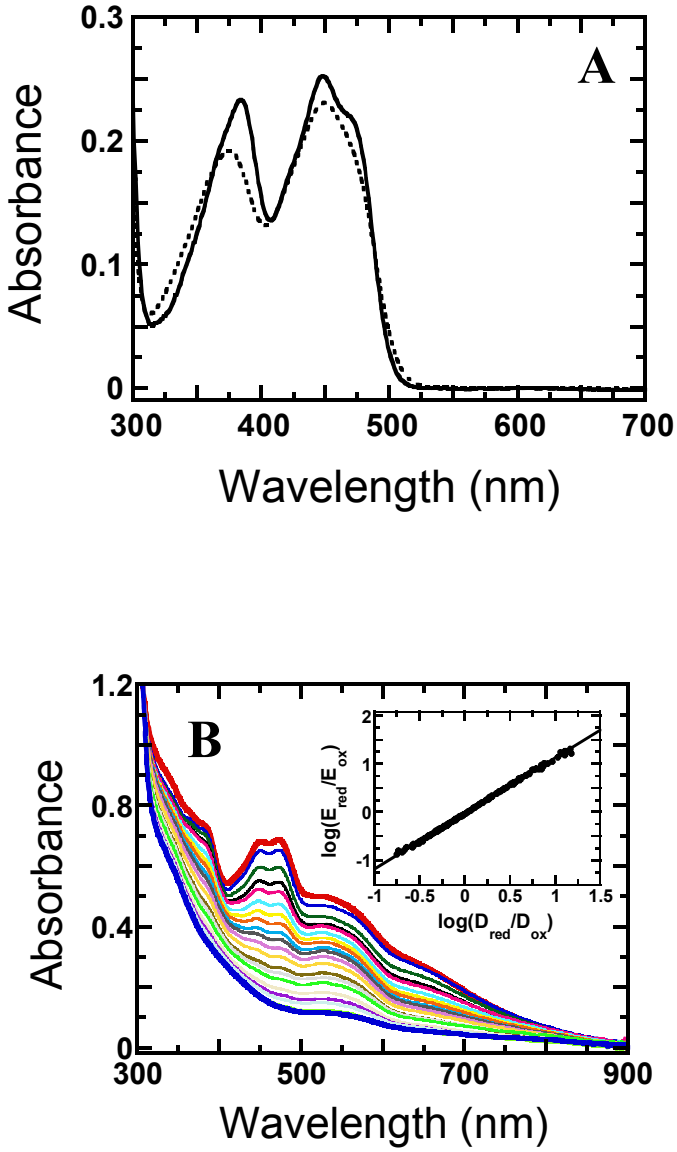

Fig. 2

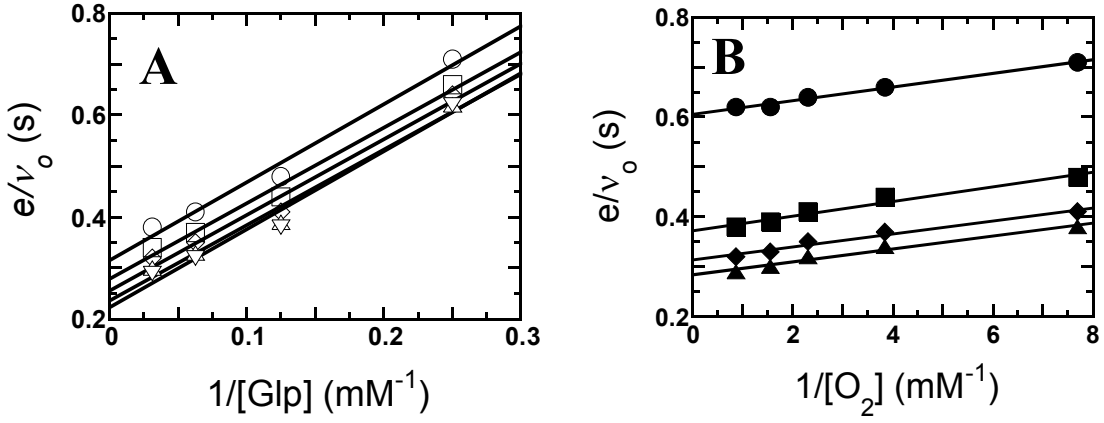

Fig. 3

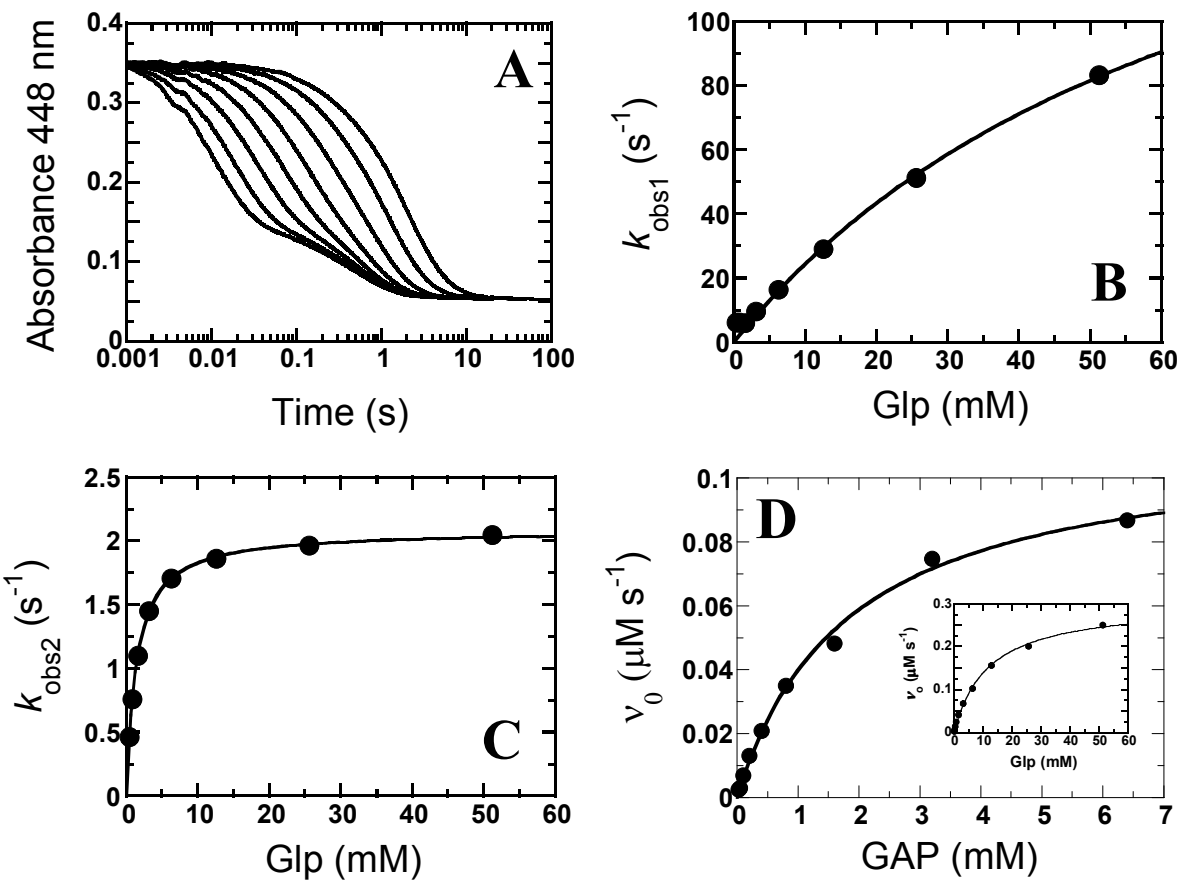
A
Absorbance 448 nm
Time (s)
B
k_{obs1} (s^{-1})
Glp (mM)
C
k_{obs2} (s^{-1})
Glp (mM)
D
v_0 ($\mu M\ s^{-1}$)
GAP (mM)
Glp (mM)

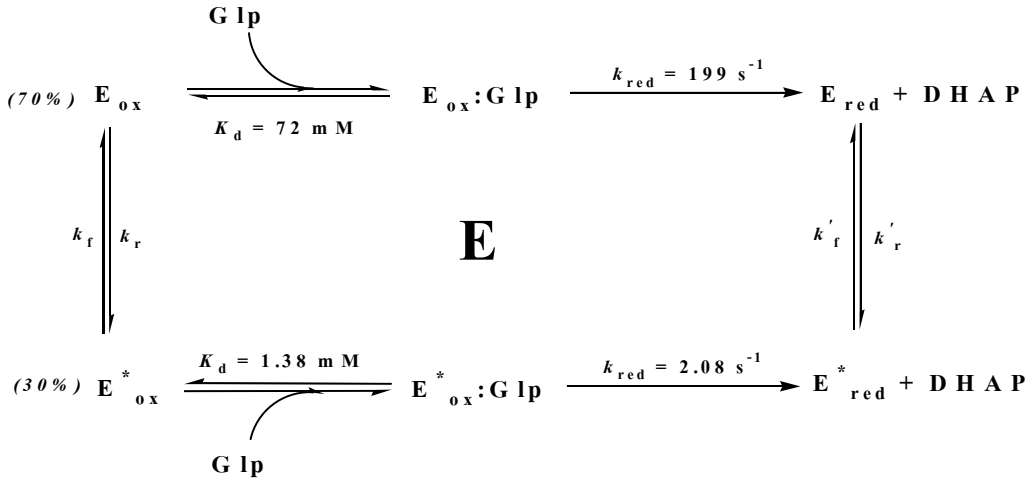
Glp
(70%) E ox
E ox:Glp
k_{red} = 199 s^{-1}
E red + DHAP
K_d = 72 mM
k_f k_r
E
k'_f k'_r
K_d = 1.38 mM
(30%) E * ox
E * ox:Glp
k_{red} = 2.08 s^{-1}
E * red + DHAP
Glp

Fig. 4

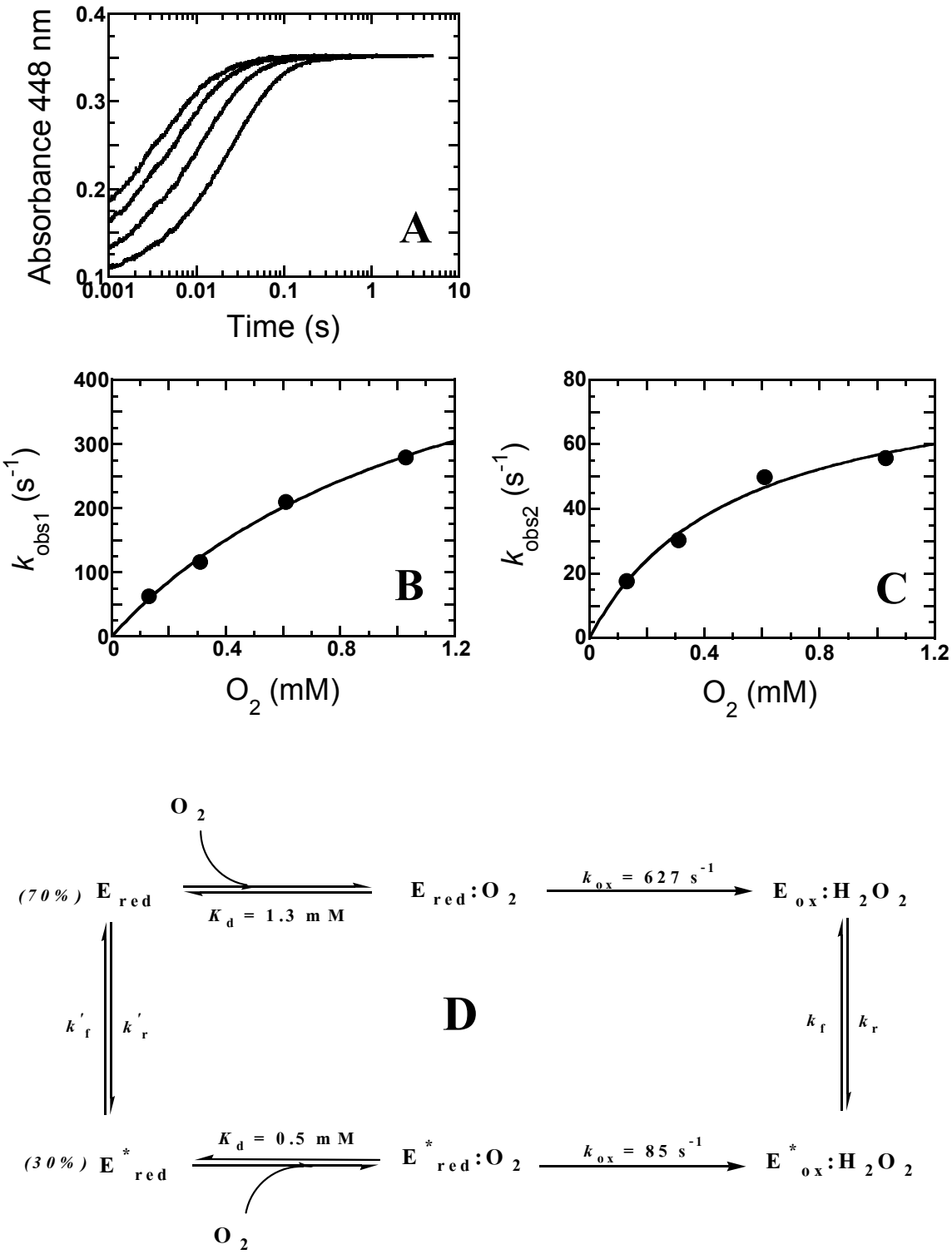
Absorbance 448 nm
Time (s)
A
k_{obs1} (s^{-1})
O_2 (mM)
B
k_{obs2} (s^{-1})
O_2 (mM)
C
(70%) E_{red}
K_d = 1.3 mM
$E_{red}:O_2$
k_{ox} = 627 s^{-1}
$E_{ox}:H_2O_2$
k'_f k'_r
D
k_f k_r
(30%) E^*_{red}
K_d = 0.5 mM
$E^*_{red}:O_2$
k_{ox} = 85 s^{-1}
$E^*_{ox}:H_2O_2$
O_2

Fig. 5

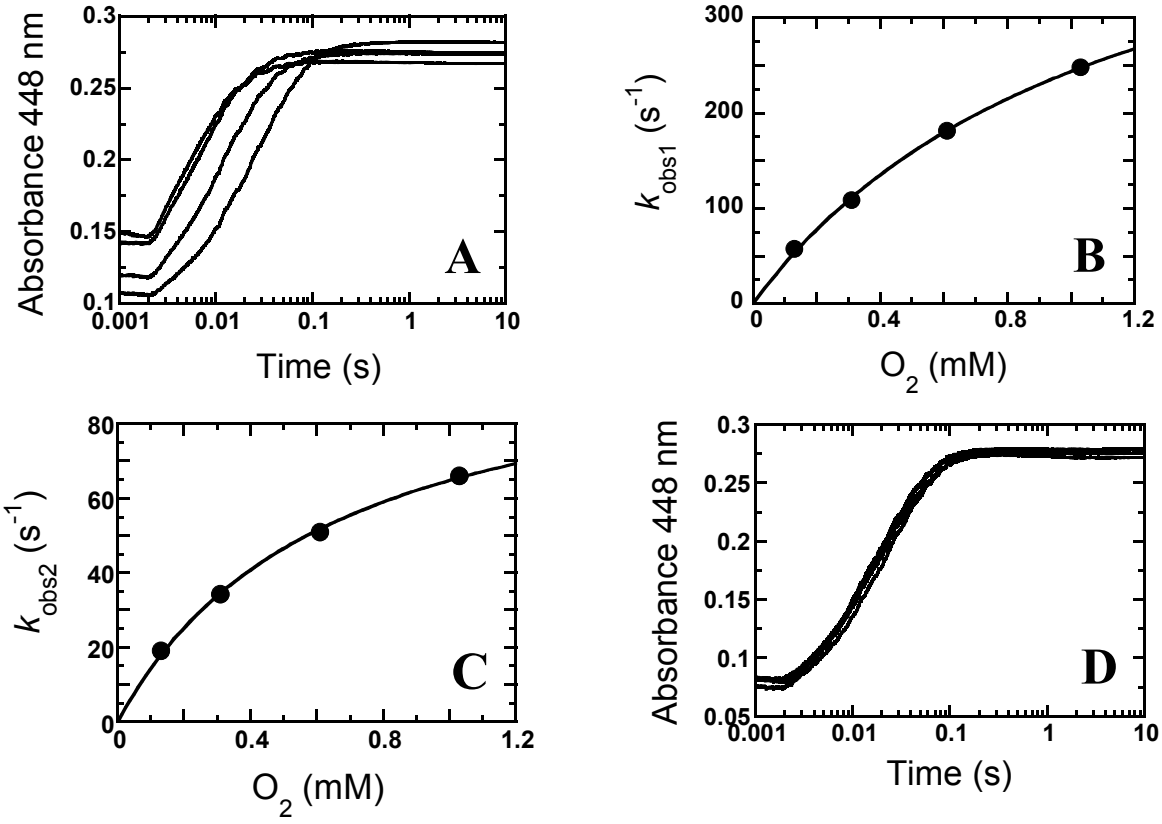
A
Absorbance 448 nm
Time (s)
B
k_{obs1} (s^{-1})
O_2 (mM)
C
k_{obs2} (s^{-1})
O_2 (mM)
D
Absorbance 448 nm
Time (s)

Fig. 6

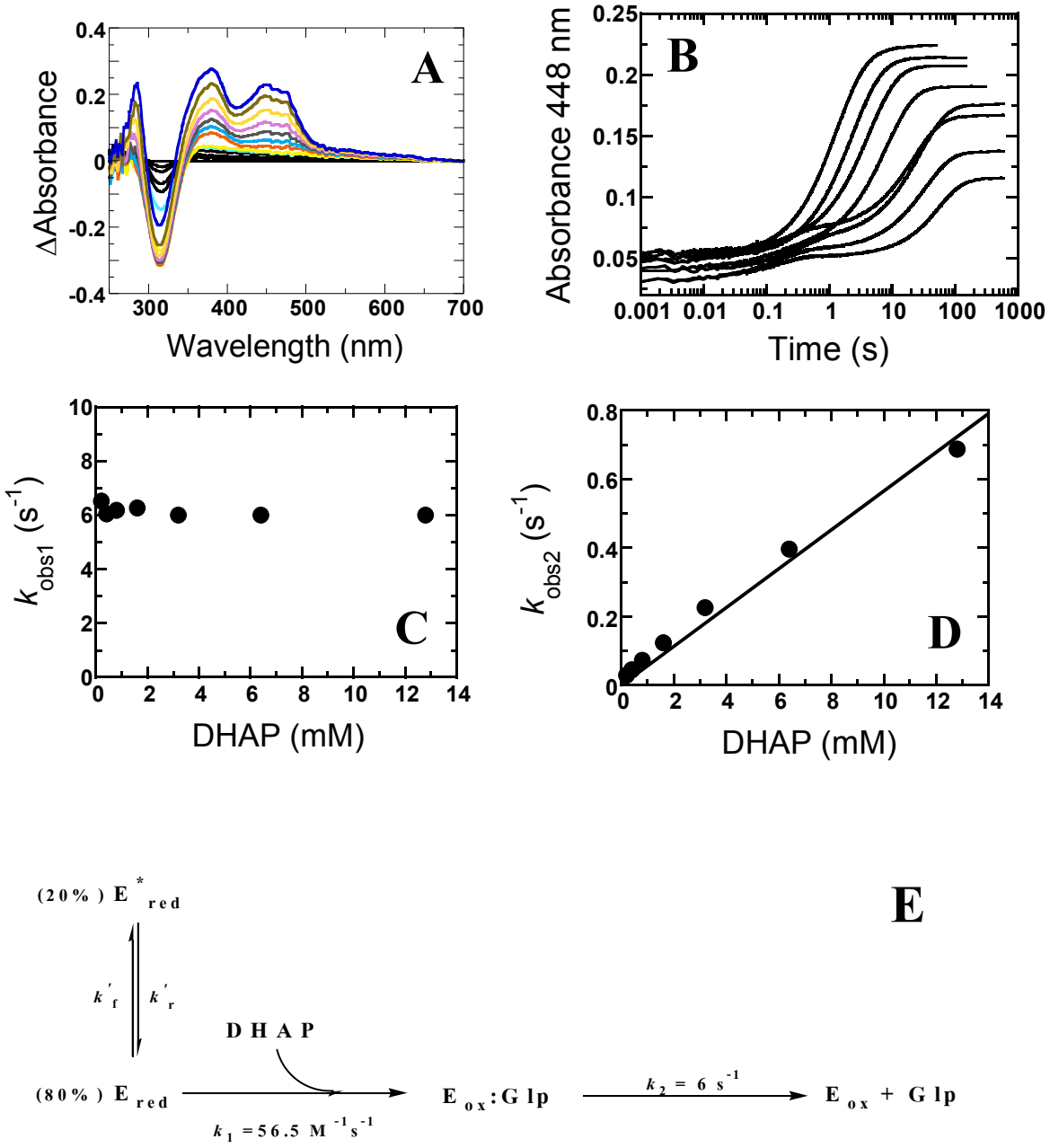
A
ΔAbsorbance
Wavelength (nm)
B
Absorbance 448 nm
Time (s)
C
k_{obs1} (s^{-1})
DHAP (mM)
D
k_{obs2} (s^{-1})
DHAP (mM)
E
(20%) E^*_{red}
k'_f
k'_r
DHAP
(80%) E_{red}
k_1 = 56.5 $M^{-1}s^{-1}$
E_{ox}:Glp
k_2 = 6 s^{-1}
E_{ox} + Glp

Fig. 7

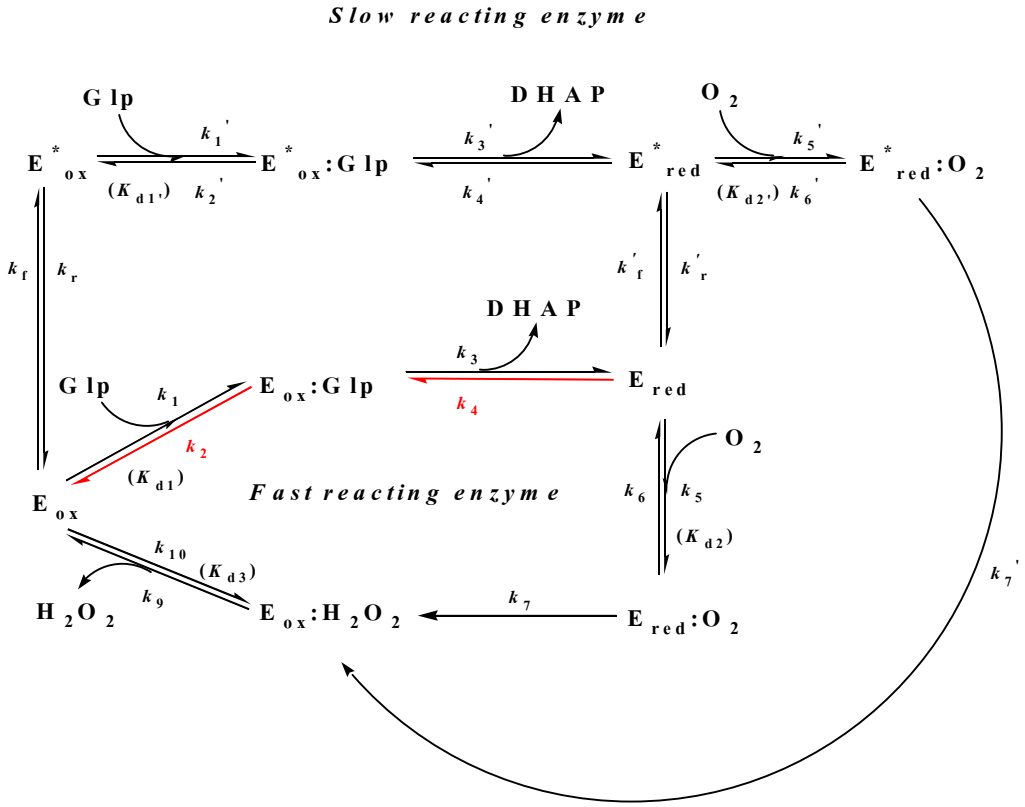
Slow reacting enzyme
Glp
DHAP
O 2
E*ox
E*ox:Glp
E*red
E*red:O2
k1'
k2'
k3'
k4'
k5'
k6'
(Kd1')
(Kd2')
kf
kr
k'f
k'r
Glp
DHAP
Eox:Glp
Ered
k1
k2
k3
k4
(Kd1)
Fast reacting enzyme
O 2
k6
k5
(Kd2)
Eox
k10
(Kd3)
k9
H2O2
Eox:H2O2
k7
Ered:O2
k7'

Kinetic Mechanism of L-α-GlycerophosphateOxidase from *Mycoplasma pneumoniae*

Somchart Maenpuen[1], Pratchaya Watthaisong[1], Pacharee Supon[1], Jeerus Sucharitakul[2], Derek Parsonage[3], P. Andrew Karplus[4], Al Claiborne[3] and Pimchai Chaiyen[5]*

[1]Department of Biochemistry, Faculty of Science, Burapha University, 169 Long-Haad Bangsaen Road, Chonburi, 20131, Thailand

[2]Department of Biochemistry, Faculty of Dentistry, Chulalongkorn University, Henri-Dunant Road, Patumwan, Bangkok 10330, Thailand

[3]Department of Biochemistry and Center for Structural Biology, Wake Forest School of Medicine, Winston-Salem, North Carolina 27157, United States

[4]Department of Biochemistry and Physics, Oregon State University, Corvallis, Oregon 97331, United States

[5]Department of Biochemistry and Center of Excellence in Protein Structure & Function, Faculty of Science, Mahidol University, Rama 6 Road, Bangkok, 10400, Thailand

Supplementary figure legends

Fig. S1. SDS-PAGE (12% (w/v)) analysis of the recombinant His_6-*Mp*GlpO after purification. Lane 1, molecular mass makers; lane 2, crude extract; lane 3, after purification by Ni-Sepharose chromatography; lane 4, after purification by SP-Sepharose chromatography. The purity of the enzyme after all processes was judged to be ~95% of total protein (20 μg) loaded.

Fig. S2. Native molecular mass of His_6-*Mp*GlpO. Native molecular mass of the purified enzyme can be determined from the calibration curve of logarithm of molecular mass of reference protein markers (empty circles); (1) ferritin (440 kDa), (2) aldolase (158 kDa), (3) bovine serum albumin (BSA; 65.4 kDa), (4) ovalbumin (48.9 kDa), (5) chymotrypsinogen A (22.8 kDa), and (6) ribonuclease A (15.6 kDa), *versus* V_e/V_o. The enzyme was eluted from Superdex S-200 HR 10/30 gel filtration chromatography at ~14 mL (Inset) and the V_e/V_o value was calculated as ~2.04 (filled circles with the arrow indicated), equivalent to the native molecular mass of 42 kDa.

Supplementary Figures

Fig. S1

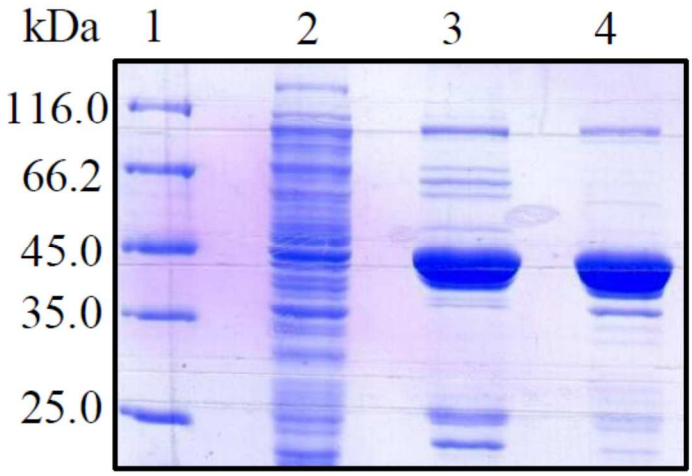

Fig. S2

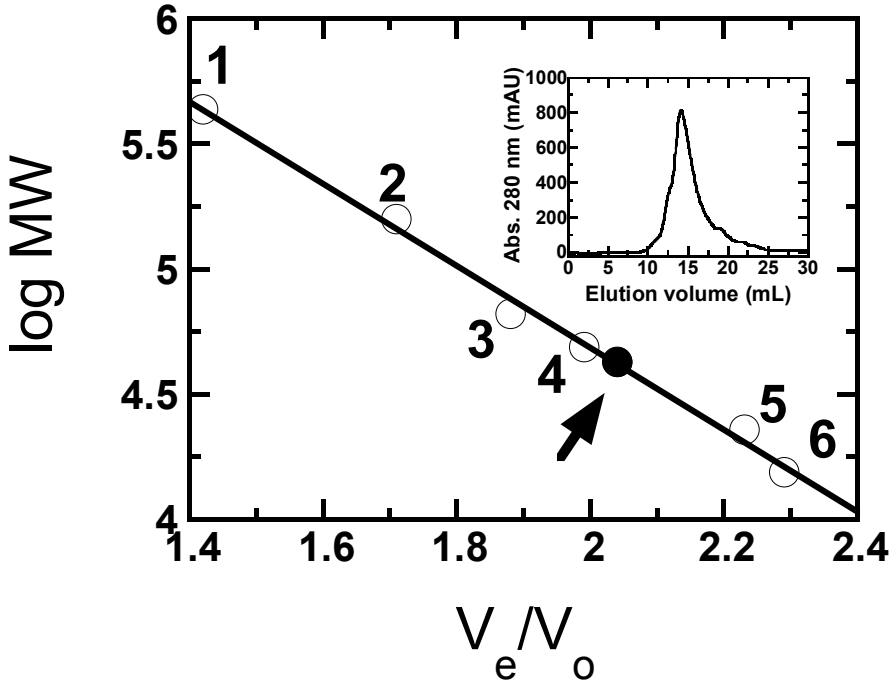
log MW
6
5.5
5
4.5
4
1.4
1.6
1.8
2
2.2
2.4
V e /V o
1
2
3
4
5
6
Abs. 280 nm (mAU)
1000
800
600
400
200
0
0
5
10
15
20
25
30
Elution volume (mL)